ELSEVIER

Journal of Alloys and Compounds 303–304 (2000) 30–36

Journal of ALLOYS AND COMPOUNDS

www.elsevier.com/locate/jallcom

Geomicrobiological controls on light rare earth element, Y and Ba distributions during granite weathering and soil formation

Anne E. Taunton, Susan A. Welch, Jillian F. Banfield*

Department of Geology and Geophysics, University of Wisconsin-Madison, Madison, WI 53706, USA

Received 16 April 1999; accepted 6 September 1999

Abstract

In this study we examine the redistribution of trivalent and tetravalent light rare earth elements (LREEs), Ba and Y during chemical weathering of granites from southern New South Wales, Australia. In essentially abiotic zones in the lower weathering profile, primary allanite is dissolved, and apatite is extensively replaced by secondary LREE lanthanide phosphates such as rhabdophane and florencite. This association is attributed to the relatively high concentrations of phosphorus at dissolving apatite surfaces and low solubility products for lanthanide phosphates. Bulk chemical data from the lower profile indicate considerable enrichment of Y, La and Nd. In contrast, in granites weathered in proximity to the soil zone, secondary lanthanide phosphates are rare and phosphate surfaces are often colonized by bacteria and fungal hyphae. Bulk chemical data show that Y, La and Nd decrease in abundance with increasing weathering. Low dissolved phosphate concentration due to microbial uptake of phosphorus suppresses secondary phosphate precipitation and also leads to dissolution of secondary lanthanide phosphates formed prior to colonization. In the most highly weathered rocks and soils, secondary phosphates are extremely rare, and only Ce oxides remain. Bulk chemical data show Ce concentrations in excess of 1200 ppm in some soils. Retention of Ce as Ce-oxides reflects the low mobility of (tetravalent) Ce under oxidizing conditions. These observations explain heterogeneities in LREE abundances in weathering profiles, development of extreme Ce anomalies, and greatly elevated concentrations of trivalent LREEs in some regions.

Keywords: REE; Phosphate; Microorganisms; Fractionation; Dissolution; Florencite

1. Introduction

Lanthanide abundances are extremely important indices of mantle and crustal geochemical evolution. To a significant extent, lanthanide distribution patterns of soils, sediments, and rocks are determined by processes occurring during chemical weathering. Lanthanide behavior under conditions near the Earth's surface is also of considerable environmental importance because lanthanides serve as geochemical proxies for actinides in contaminated sites.

During early stages of crystallization of igneous rocks, lanthanides (rare earth elements, REE) concentrate in the melt phase. In most rocks, REE behavior is largely controlled by accessory minerals, including phosphates such as monazite (REE, Th)PO_4 and silicates such as allanite (Ca, Ce, La)$_3$(Fe^{2+}, Fe^{3+})$Al_2O(SiO_4)(Si_2O_7)(OH)$. When exposed to conditions near the Earth's surface, minerals such as allanite weather, releasing REE that may go into solution or precipitate as a variety of secondary phases.

It has been suggested that the clay size fraction controls the distribution of lanthanides in some weathered materials [1–4]. However, most studies do not differentiate between lanthanides substituted into silicate clay structures, adsorbed onto their surfaces, or partitioned into coexisting finely crystalline accessory minerals.

There is close coupling between the geochemistry of lanthanides and phosphate over a wide range of Earth conditions. Monazite (REE, Th)(PO_4) crystallization at high temperature may control REE distributions in melts, and a variety of phosphates may host lanthanides at low temperatures [5]. The apatite group [$Ca_5(PO_4)_3$(F, Cl, OH)], the primary phosphate minerals in igneous rocks, typically only contain on the order of thousands of ppm REE. However, since it is the primary inorganic source of dissolved phosphate during weathering of igneous and metamorphic rocks, apatite can localize precipitation of secondary lanthanide phosphates [3,6]. For example, prior studies have demonstrated redistribution of REE released

---

*Corresponding author.

E-mail address: jill@geology.wisc.edu (J.F. Banfield)

PII: S0925-8388(00)00597-1

by allanite weathering form secondary phosphates that crystallize on etched apatite surfaces [6].

Secondary phosphate phases can accommodate a variety of high atomic number elements, including Ba and Pb [7,8]. Based on the very low solubility products (rhabdophane K_{sp}~10^{-26}; [9]), phosphate addition has been proposed as a method for immobilization of heavy metals and radionuclides at contaminated sites [e.g. 10,11]. However, this strategy derives from only inorganic considerations. Given that secondary phosphates may be the primary inorganic reservoir for phosphorus needed by the biosphere, microbial controls on secondary phosphate stability must also be considered.

Phosphorus is a biologically essential element. It is needed for formation of adenosine triphosphate (ATP, the molecule central to biological energy generation), DNA, RNA, phospholipids and other major cell constituents. In the oceans, soils and sediments, phosphorus is often a limiting nutrient for organisms. Consequently, it is probable that microorganisms have evolved strategies for solubilizing inorganic phosphates. In fact, microbial solubilization of insoluble phosphates has been reported [12–14]. Further analyses of microbial contributions to secondary phosphate stability are needed before the probable success of long term immobilization of contaminants by phosphate amendments can be predicted.

In this paper we examine the reasons for highly variable LREE, Y and Ba distributions in weathered rocks and consider the roles microorganisms play in determining secondary phosphate stability.

2. Methods

Forty-five samples were collected from a granite weathering profile exposed in a road cut on the Snowy Mountains Highway between Nimitabel and Bemboka, in Southeastern New South Wales, Australia. The lower portion of the profile, approximately 6 m below the soil zone, was first sampled in 1983, soon after the road cut was created [15]. In the current study, samples ranging from slightly weathered rock to granitic soil were collected in 1998 and 1999. The sample locations run a vertical weathering gradient from the top of the profile through the soil zone to slightly weathered rock within 3 m of the soil zone. Rock samples were collected and placed in sterile plastic bags. Saprolite and soil samples were asceptically collected using autoclaved spatulas and placed in sterile bags or falcon tubes. Unlike the prior study, the samples targeted in the upper profile show clear evidence of mineral surface colonization by organisms, including plants. Soils show loss of the granite texture characteristic across the majority of the weathering profile, and contain abundant roots and some organic detritus.

Many apatite crystals in the granite occur as inclusions within the mica group mineral, biotite. Consequently, biotite crystals were handpicked from each sample, split, and mounted on aluminum stubs with carbon tape for scanning electron microscope (SEM) analyses and energy-dispersive X-ray spectrometry (EDX). Most samples were coated with carbon to eliminate peak overlap in EDX, however some were coated with platinum for high resolution SEM. Electron microprobe (EMP) analyses were obtained from several samples. Bulk rock chemical data for the profile were obtained by X-ray fluorescence analyses conducted at the Australian National University, Canberra, Australian Capital Territory.

3. Results

3.1. Field emission SEM, EMP, and EDX analyses

Increasing weathering, as indicated by an increase in the alteration of surrounding biotite to halloysite and a decrease in the cohesiveness of samples at the hand specimen scale, correlates with an increase in apatite etching and a corresponding decrease in the amount of apatite. Fig. 1 is a field-emission SEM image of a sample from slightly weathered granite. The biotite contains an apatite crystal with its *c* axis horizontally oriented. Space at the end of the crystal has been created by apatite dissolution. The prominent spires (parallel to *c*) remaining on the termination of the apatite crystal are attributed to heterogeneous etching.

Secondary phases occur on weathered apatite. The abundance and morphology of these phases varies considerably within the profile. The horizontal, upper surface of the apatite in Fig. 1 is coated with crystals. EDX analyses show that these crystals are enriched in LREEs, especially La and Ce. In some cases, secondary phosphates

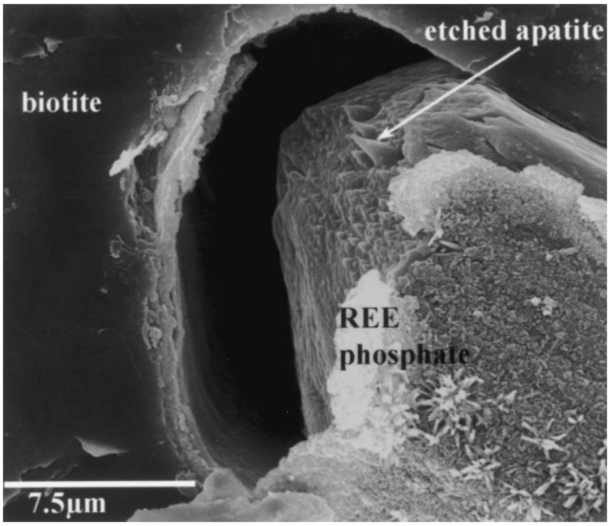

Fig. 1. Field emission SEM image of etched apatite coated with secondary phosphates.

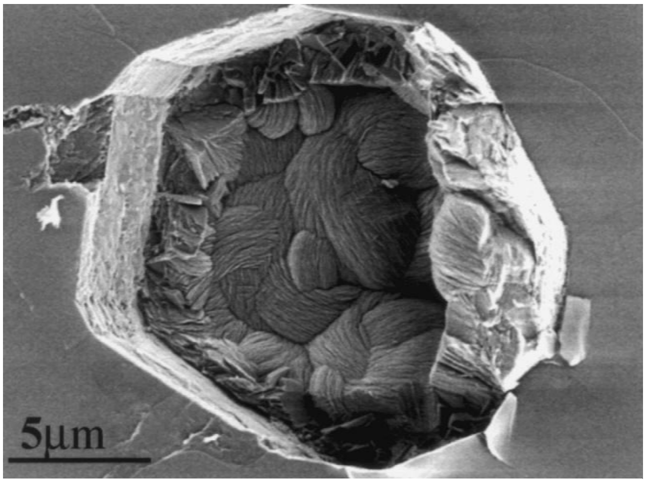

Fig. 2. Field emission SEM image of relict apatite pit with radiating florencite crystals.

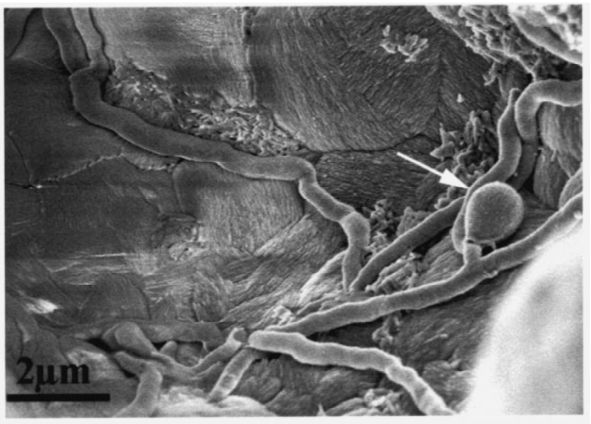

Fig. 4. Field emission SEM image of fungal hyphae with a fruiting body (indicated by arrow) resting on florencite in a relict apatite pit. Hyphae are concentrated inside the pit.

also develop as coatings or thin rinds. Elsewhere, secondary phosphates occur as rounded aggregates, sometimes with distinct 'donut-shaped' forms.

Fig. 2 is a field-emission SEM image of a pit exhibiting the characteristic hexagonal shape of apatite (oriented with the c̲ axis normal to the page). The pit contains a secondary mineral with an Al, P, Ba, Ca, La, and Ce-rich composition (Fig. 3). High-resolution characterization of the rounded aggregates (especially the broken aggregates on the left side of the pit) indicates they consist of radiating elongate crystals 3 to 5 μm in length. In this case, no primary apatite is apparent. In other samples, these aggregates coexist with etched apatite.

Lanthanide phosphates are always associated with apatite pits, but their abundance in these pits is heterogeneous. Lanthanide phosphates are less common in the upper regions (closer to the soil zone) than in the lower region of the profile. Secondary phosphates occasionally coexist with titanium dioxide, iron oxides or oxyhydroxides, and halloysite (these minerals crystallize from elements released by weathering of surrounding biotite and feldspar). In highly weathered granite, pits are typically free of phosphate minerals, and the only abundant secondary mineral present is halloysite.

Fungal hyphae and bacteria are associated with secondary phosphates in some relict apatite pits (Figs. 4 and 5). Fig. 4 is a field-emission SEM image of fungal hyphae on REE-Al phosphate (note the same texture in the mineral substrate in Fig. 2). A 1.5 μm reproductive body is apparent on the 0.5 μm diameter fungal hyphae on the right hand side of the image (some dehydration has occurred as a result of the high vacuum in the SEM).

Fig. 5 shows a field-emission SEM micrograph of bacteria in a relict apatite pit that contains abundant secondary titanium dioxide. The bacteria are ~1 to 2 μm in length and ~0.3 μm in diameter. A larger, ~3 μm diameter cell (possibly a fungal hyphae) is also evident in the middle of the pit. The microorganisms are concentrated

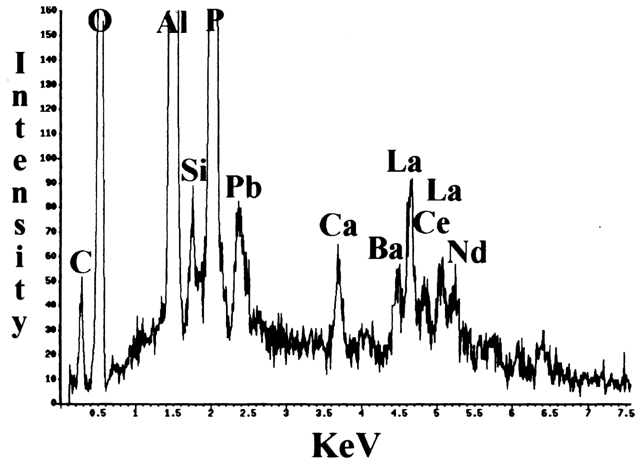

Fig. 3. Energy-dispersive X-ray analysis of florencite shown in Fig. 2.

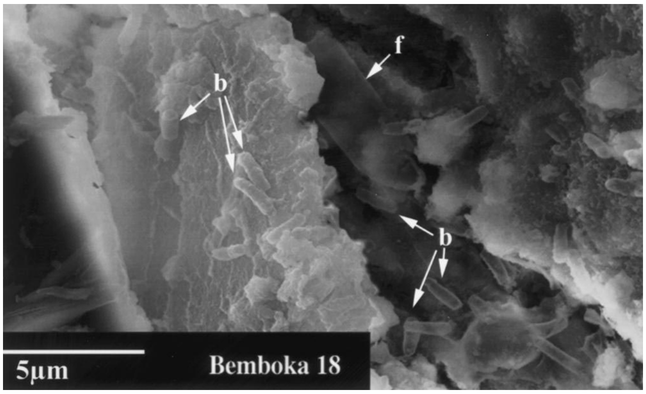

Fig. 5. Field emission SEM image of bacteria (b) and fungal hyphae (f) in relict apatite pit. Microorganisms are not found on surrounding biotite.

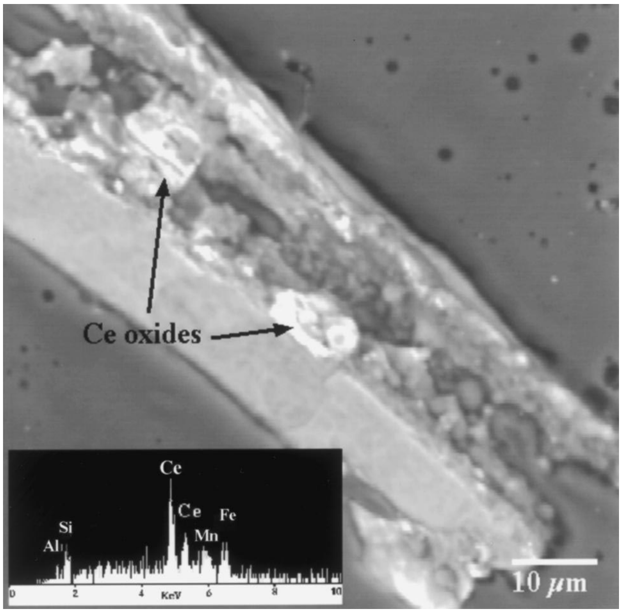

Fig. 6. Backscattered electron image of CeO_2 in relict apatite pit. The energy-dispersive X-ray spectra of high atomic weight elements is shown on left hand side of the image.

within the pit and are not abundant on the surrounding biotite.

A backscattered electron image from a thin section of a sample from a soil region of the profile shows high atomic number elements associated with relict apatite pits (Fig. 6). The EDX spectra (lower left corner of Fig. 6) indicates abundant Ce and no detectable phosphorus. We infer the crust to be Ce-oxide or oxyhydroxide. Ce-oxides or Ce-oxyhydroxides were also detected by EDX analyses of secondary minerals in a hexagonal pit formed by dissolution of apatite (Fig. 7). At higher magnification, mineralized cells are apparent on the Ce-oxide crust (Fig. 8).

In addition to identification by morphology, samples were stained with 4',6-diamidino-2-phenylindole (DAPI). This stain fluoresces when bound to the DNA of cells. Imaging by epifluorescence microscopy confirmed high abundances of cells in some relict apatite pits.

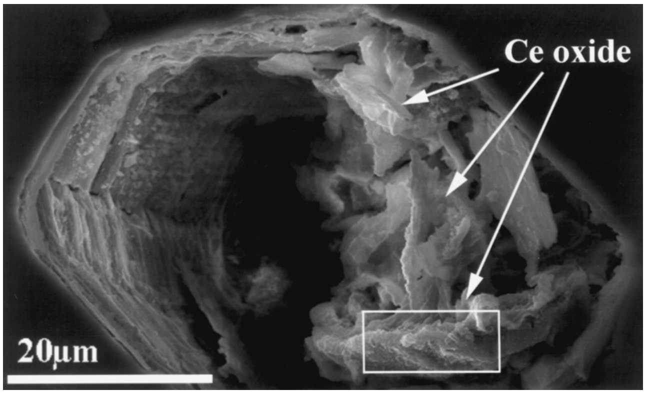

Fig. 7. Low magnification field emission SEM image of an apatite pit containing CeO_2.

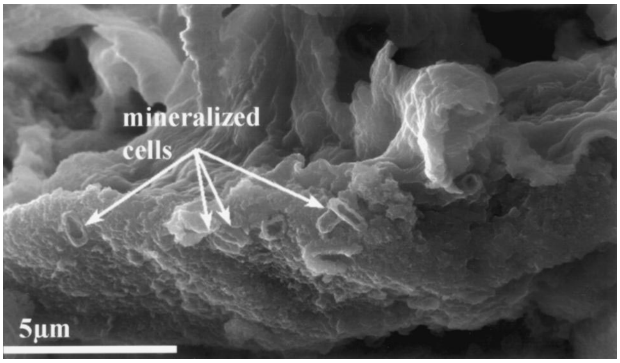

Fig. 8. Higher magnification field emission SEM image of boxed area of crust in Fig. 7, showing mineralized microorganisms associated with the CeO_2 products.

3.2. Bulk rock chemistry

Granite weathering in this profile occurs under oxidizing conditions, so increasing weathering (as indicated by decrease in bulk density, see [15]) correlates with decrease in abundance of FeO and increase in abundance of Fe_2O_3. In highly weathered samples, density can not be used as an index of weathering because sample volumes do not remain constant at high degrees of alteration. Consequently, we use wt% Fe_2O_3 as an index of weathering. Fig. 9 a,b show several LREEs, Y and Ba concentrations in the lower profile (1983 [6]) and new data for concentrations in the upper region (1999) plotted against wt% Fe_2O_3. In contrast to the lower weathered granite profile, the upper weathered granite and soils show marked La depletion along with a depletion in Nd, Y, and Ba. However, Ce increases in the both the lower and upper portions of the profile. Ce abundances in soils are highly variable, and Ce concentrations range up to more than twelve times those of fresh rock.

4. Discussion

Allanite is the primary host for REEs (especially lower atomic number REE) in the granite. REE released by allanite dissolution precipitate as secondary phosphates when solutions encounter concentrations of dissolved phosphorus in proximity to apatite dissolution sites. Based on their compositions and electron and X-ray diffraction patterns, Banfield and Eggleton [6] identified secondary phosphate minerals in the lower profile as rhabdophane $(Ce, La, Nd)PO_4 \cdot H_2O$ and florencite $(Ce, La)Al_3(PO_4)_2(OH)_6$. The composition of the dominant phosphate-bearing secondary mineral in the upper weath-

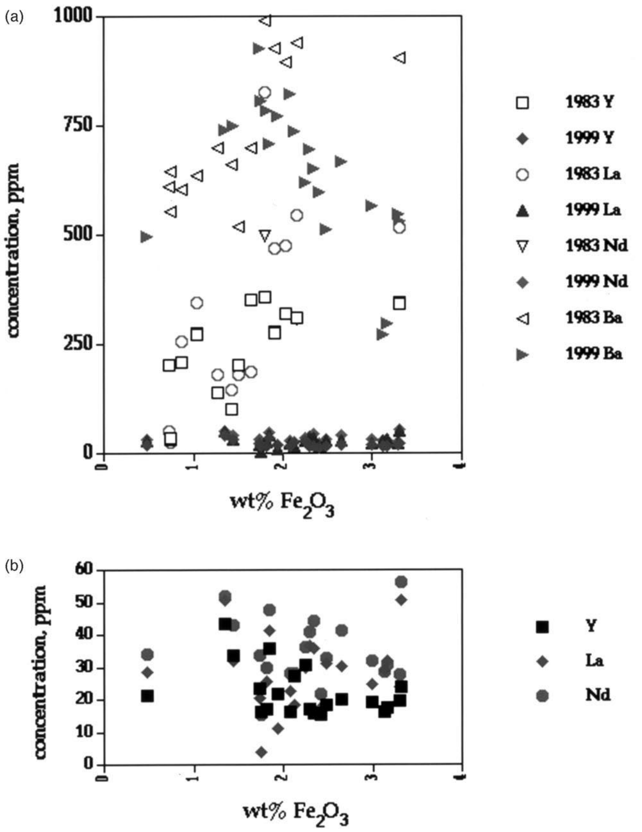

Fig. 9. (a) Geochemical analyses of several La, Nd, Y, and Ba in lower (1983) and upper (1999) regions of the granite weathering profile plotted against wt% Fe_2O_3, which increases in abundance with increased degree of weathering. La, Nd, Y and Ba are enriched in the lower region but depleted in the upper region of the profile. (b) enhancement of lower region of Fig. 9a. La, Nd, and Y are shown to decrease in the upper region of the weathering profile.

ered granite and soil is consistent with florencite (though some rhabdophane may also be present).

Whole rock chemical data for the lower profile showed that all REE except Ce are enriched four to thirteen times (after correction of weight-based abundances to remove apparent concentration effects due to change in rock density) compared to fresh rock [6]. Strong REE enrichments in slightly weathered samples (3% decrease in density) persist in very highly weathered samples. Thus, under conditions encountered in the lower profile, secondary phosphates are insoluble.

SEM characterization of samples from the upper profile and soil showed much lower abundance of florencite±rhabdophane compared to the lower profile. This result is consistent with bulk chemical analyses, which indicated loss of Y, Ba, and LREEs, except Ce from the upper regions of the profile with increasing weathering (Fig. 9a, b). These data imply that lanthanide phosphates are not insoluble in the upper profile. Thus, we infer that secondary lanthanides added to the lower profile are derived from the upper profile and soil zone. This is consistent with results of Banfield and Eggleton [6], which demonstrated minimal fractionation across the lanthanide series (except for Ce) in the lower profile, indicating lanthanides were derived from surrounding granite.

The explanation for inhibition of crystallization of secondary phosphates, or solubilization of these phases in the upper profile, may be related to microbial processes. In the upper profile, local colonies of bacterial and fungal cells are common. However, readily bioavailable phosphorus from organo-phosphates is limited by scarcity of organic detritus. Under these conditions, the moderately soluble apatite dissolves. Resistant secondary phosphate minerals then represent the remaining inorganic phosphate reservoir. This leads to colonization of secondary phosphate surfaces when sufficient porosity and permeability are created by granite weathering.

One way in which microorganisms can lead to a lower abundance of secondary phosphates in the upper profile may be through uptake of dissolved phosphate, which inhibits secondary phosphate crystallization. In contrast, solutions in the lower profile remain saturated with respect to secondary phosphates because the biological sink for phosphorus is minimal (phosphate requirements of the minimal biomass in this zone can be met by apatite dissolution).

The association between cells and secondary mineral surfaces in the upper profile suggests that another factor contributing to low lanthanide phosphate abundance in highly weathered granite is microbially-mediated dissolution. Microorganisms may enhance dissolution of earlier-formed secondary phosphates by changing the solution saturation state through microbial uptake of phosphorus. Additionally, dissolution may be promoted by the release of complexing agents, organic acids, or enzymes (perhaps analogous to alkaline phosphatases used by microorganisms to extract phosphorus from organic compounds). Microbial solubilization of secondary phosphates has not been studied to date. However, Welch et al. [16] demonstrated that apatite dissolution is greatly accelerated in solutions containing oxalate, acetate, and actively metabolizing heterotrophic cells. Because the dissolution rate of apatite is strongly pH dependent, the predominant effect may be generation of acidity.

Cerium behavior differs from that of other LREEs. Weight-based abundances in the lower profile increased by a factor of 1.4 with increased weathering, and volume-based abundances were nearly constant. Thus, Ce is relatively immobile in the lower profile [6]. Samples from the upper profile are so extensively weathered that density measurements are meaningless (due to compaction following removal of soluble components). When REE abundances are plotted using Fe_2O_3, Ce behavior parallels that of the lower profile, except in the soil zone. The soil zone shows Ce enrichment in excess of twelve times the weight-based abundance of unweathered rock (Fig. 10). This either can be attributed to Ce mobilization and reprecipitation, or to twelve times compaction in the soil zone. The

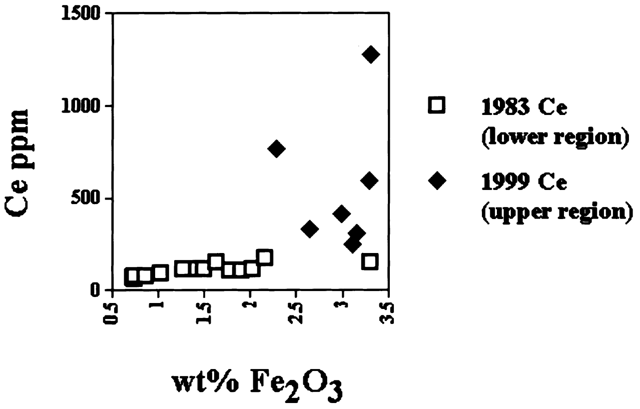

Fig. 10. Geochemical analyses of Ce in lower weathered granite (1983) and upper weathered granite and soil (1999). Ce is immobile in the lower region, and concentrated in the soil zone.

former explanation is improbable, given consistent retention of Ce at near-initial levels throughout the weathering profile, presumably due to Ce oxidation and precipitation of tetravalent Ce- oxides. A twelve fold compaction (implying removal of~92% of original constituents) is surprising, but perhaps not unexpected at this old, deeply weathered site. Unfortunately, other typically relatively immobile elements such as Zr in zircon and Ti in ilmenite and rutile exhibit considerable mobility in the soil and near-soil zones, so compaction values can not be independently verified.

Bulk Ce data conceal interesting heterogeneities in Ce distribution within individual samples. Two different types of florencite were identified. Type 1 florencite is clearly depleted in Ce compared to La, yet Type 2 florencite contains comparable La and Ce abundances. This phenomenon was noted previously in the lower profile [6], but not explained. The lack of fractionation of Ce from other lower atomic number REEs in Type 2 florencite suggests that, like the other REEs, Ce was solubilized as a trivalent cation during allanite dissolution. This implies that in the early stages of weathering of regions containing Type 2 florencite, conditions were relatively reducing. This is not unexpected, given low porosity, limited fluid flow, and adjacent oxygen-consuming weathering reactions involving silicate minerals. Where solutions are more oxygenated (e.g., more porous regions with enhanced fluid flow), immobilization of Ce in its tetravalent state is expected. In this case, secondary phosphates will be characterized by low Ce concentrations. The existence of two florencite compositions implies spatially heterogeneous solution chemistry during early weathering.

Lanthanides are important geochemical tracers used to study the origin of sediments and crustal evolution. Cerium anomalies associated with sediments may originate in weathering reactions. Erosion of highly weathered materials, especially these clay-rich soils, would produce a sediment with a strong positive Ce anomaly. Erosion products derived from the upper portion of the profile would be characterized by a small positive Ce anomaly, whereas sediments derived from the lower profile would be characterized by a large negative Ce anomaly. If further studies show heterogeneities such as those reported here are common in weathered granites, sediment lanthanide distribution patterns may provide insights into characteristics of the source region, including the redox state of the profile during weathering.

Data presented in the paper have some relevance to understanding the roles of natural inorganic and microbial processes in controlling heavy metal distributions in contaminated sites. Although not perfect analogues, our results may provide some insights into how the geochemically similar actinide group elements (including Pu) will be distributed in weathered rocks and soils. Specifically, these data suggest that both biological and inorganic factors may dramatically influence the precipitation and dissolution of actinide phosphates.

Acknowledgements

Microscopy was carried out at the NASA-Johnson Space Center, the Australian National University (ANU), and The Materials Science Center, University of Wisconsin-Madison. Dr. David McKay and Lou Hulse are thanked for providing access to NASA microscope facilities. We extend thanks to Sally Stowe for providing access to microscopy facilities at ANU, and Roger Heady for assistance with microscope operation. Jeffrey Brownson and Geoffrey Olley are thanked for their assistance with preparation of rocks for XRF analysis. Dr. Bruce Chappell was the analyst responsible for generation of bulk chemical analyses. Comments of two anonymous reviewers are acknowledged. This research was supported by grants from the National Science Foundation (EAR-9706382) and the Department of Energy (DEFG02-93ER14328).

References

[1] I.R. Duddy, Chem. Geol. 30 (1980) 363–381.
[2] K.B. Esser, J.G. Bockheim, P.A. Helmke, Soil Sci. 152 (1991) 340–350.
[3] H.G. Dill, A. Fricke, K.H. Henning, Appl. Clay Sci. 10 (1995) 231–245.
[4] L. Minarik, A. Zigova, J. Bendl, P. Skrivan, M. Stastny, Sci. Total Environ. 215 (1998) 101–111.
[5] K.A. Vlasov (Ed.), Mineralogy of the Rare Elements, Geochemistry and Mineralogy of Rare Elements and Genetic Types of Their Deposits, Vol. III, Israel Prog. For Sci. Trasl, Jerusalem, 1966, p. 945, Translated by Z. Lerman.
[6] J.F. Banfield, R.A. Eggleton, Clays and Clay Minerals 37 (1989) 113–127.
[7] S.M.B. De Oliveira, R.A.L. Imbernon, J. S. Am. Earth Sci. 11 (1998) 379–388.

[8] K. Norrish, in: Trans. 9th Congr. Int. Soil Sci. Soc, Vol. 2, 1968, pp. 713–723, Adelaide.

[9] R.G. Jonasson, G.M. Bancroft, H.W. Nesbitt, Geochim. Cosmochim. Acta 49 (1985) 2133–2139.

[10] Qy Ma, S.J. Traina, T.J. Logan, and J.A., Environ. Sci. Tech. 9 (1993) 1803-1810.

[11] V. Laperche, T.J. Logan, P. Goldstein, S.J. Traina, Environ. Sci. Tech. 10 (1997) 2745–2753.

[12] D.C. Di Simine, J.A. Sayer, G.M. Gold, Biol. Fert. Soils 28 (1998) 87–94.

[13] P. Illmer, A. Barabato, F. Schinner, Soil Biol. Biochem. 27 (1995) 265–270.

[14] J.A. Sayer, M. Kierans, G.M. Gold, Fems Microbiol. Lett. 154 (1997) 29–35.

[15] J.F. Banfield, The mineralgy and chemistry of granite weathering: M. Sc. Thesis, Australian National University, Canberra Australia, 1985.

[16] S.A. Welch, A.E. Taunton, J.F. Banfield. The role of microbial metabolites in apatite dissolution kinetics. In prep.